Controllable synthesis of Ni_3S_2@MOOH/NF (M = Fe, Ni, Cu, Mn and Co) hybrid structure for efficient hydrogen evolution reaction

Xiaoqiang Du[a*], Guangyu Ma[a], Yanhong Wang[a], Xinghua Han[a] and Xiaoshuang Zhang[b]

a. School of Chemical Engineering and Technology, North University of China, Taiyuan 030051, People's Republic of China. E-mail: duxq16@nuc.edu.cn

b. School of Science, North University of China, Taiyuan 030051, People's Republic of China.

DFT calculation

The DFT calculations were performed using the Cambridge Sequential Total Energy Package (CASTEP) with the plane-wave pseudo-potential method. The geometrical structures of the (111) plane of Ni_3S_2, the (003) plane of NiOOH, and (010) plane of FeOOH were optimized by the generalized gradient approximation (GGA) methods. The Revised Perdew-Burke-Ernzerh of (RPBE) functional was used to treat the electron exchange correlation interactions. A Monkhorst Pack grid k-points of 6*6*1 of Ni_3S_2, NiOOH, Ni_3S_2@NiOOH and Ni_3S_2@FeOOH, a plane-wave basis set cut-off energy of 480 eV were used for integration of the Brillouin zone. The structures were optimized for energy and force convergence set at 0.05 eV/A and 2.0×10^{-5} eV, respectively. The vacuum space was up to 0.002 A to eliminate periodic interactions.

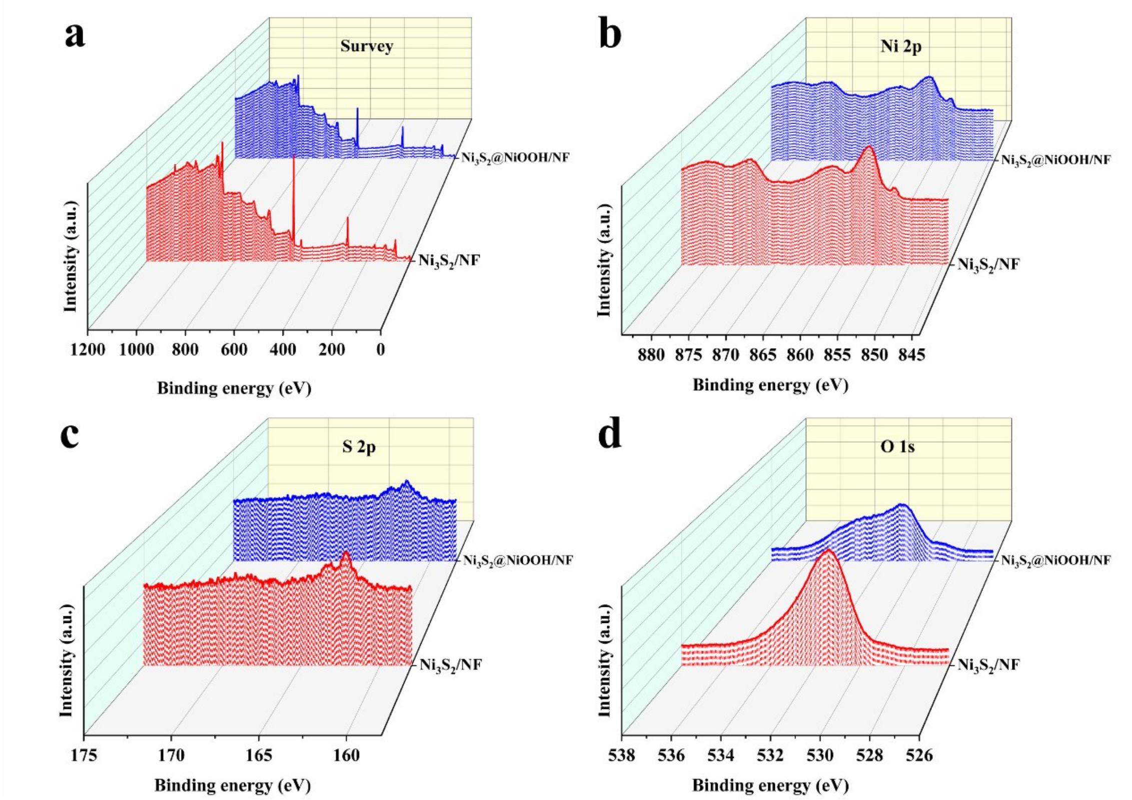

Fig. S1 (a-d) The XPS spectra of Ni_3S_2/NF and Ni_3S_2@NiOOH/NF catalysts, including full scan spectrum (a) and the high-resolution spectra of Ni 2p (b), S 2p (c), O 1s (d).

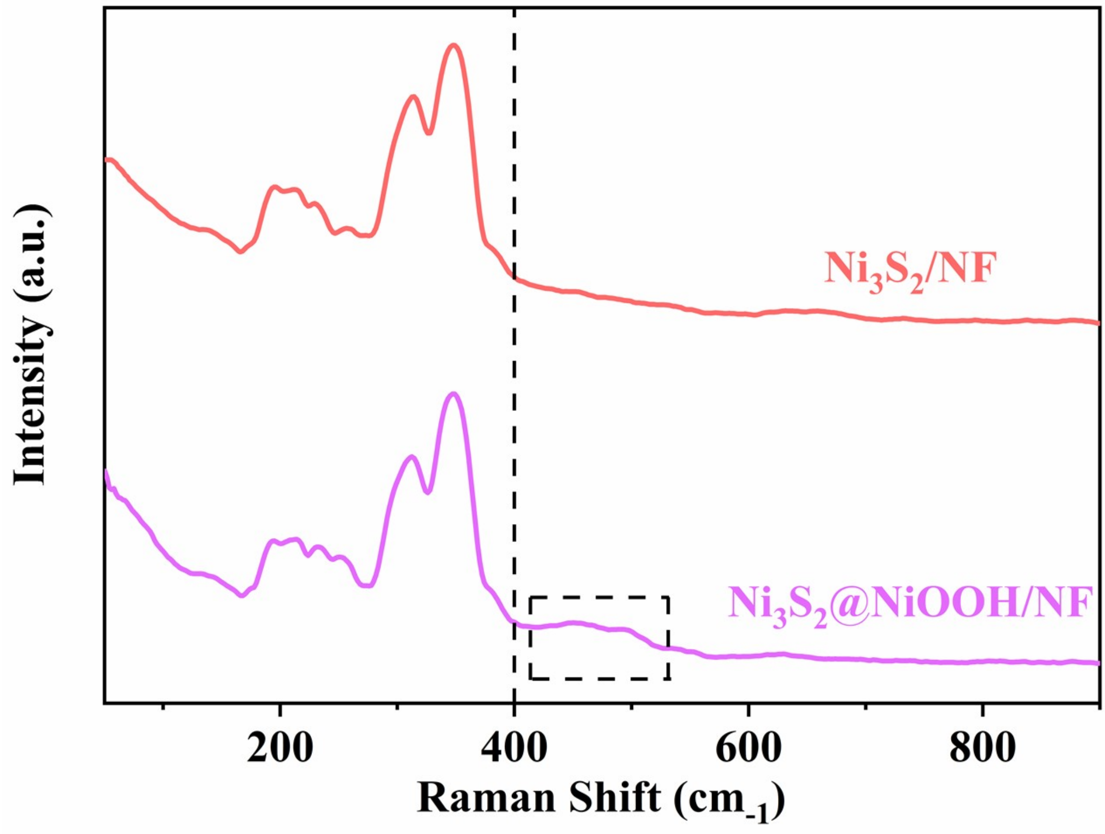

Fig. S2 The Raman spectra of Ni_3S_2/NF and Ni_3S_2@NiOOH/NF catalysts.

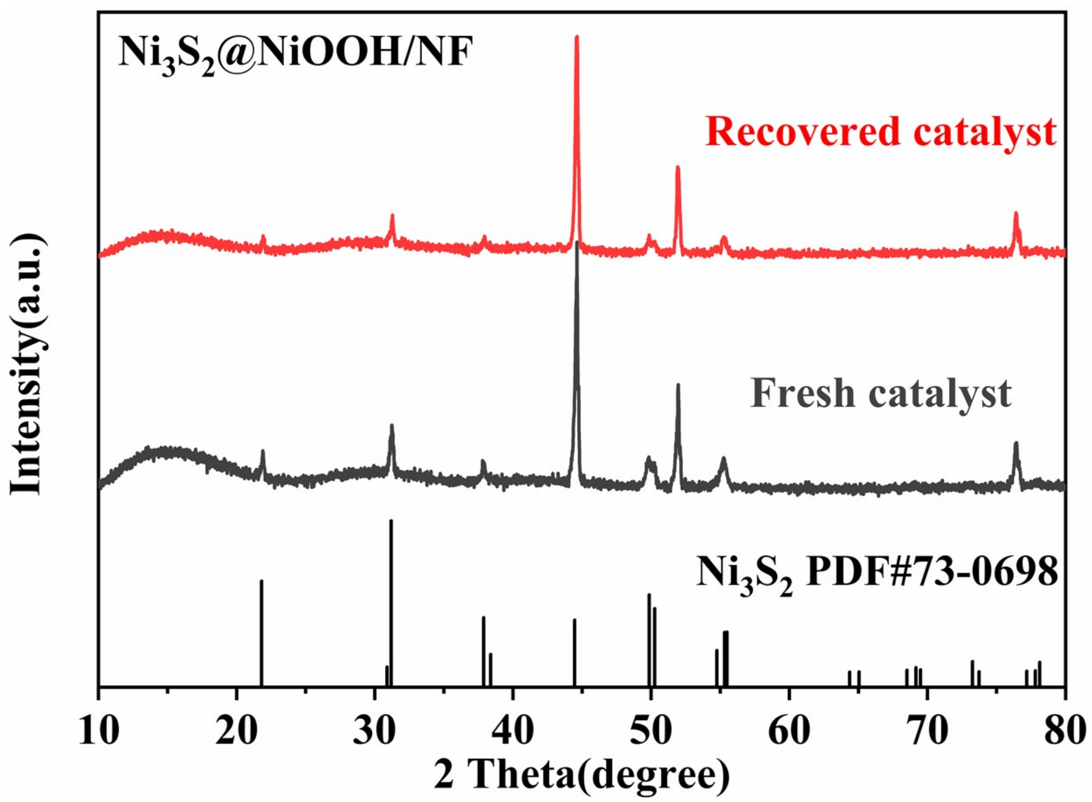

Fig .S3 The XRD patterns of Ni_3S_2@NiOOH/NF before and after HER stability test.

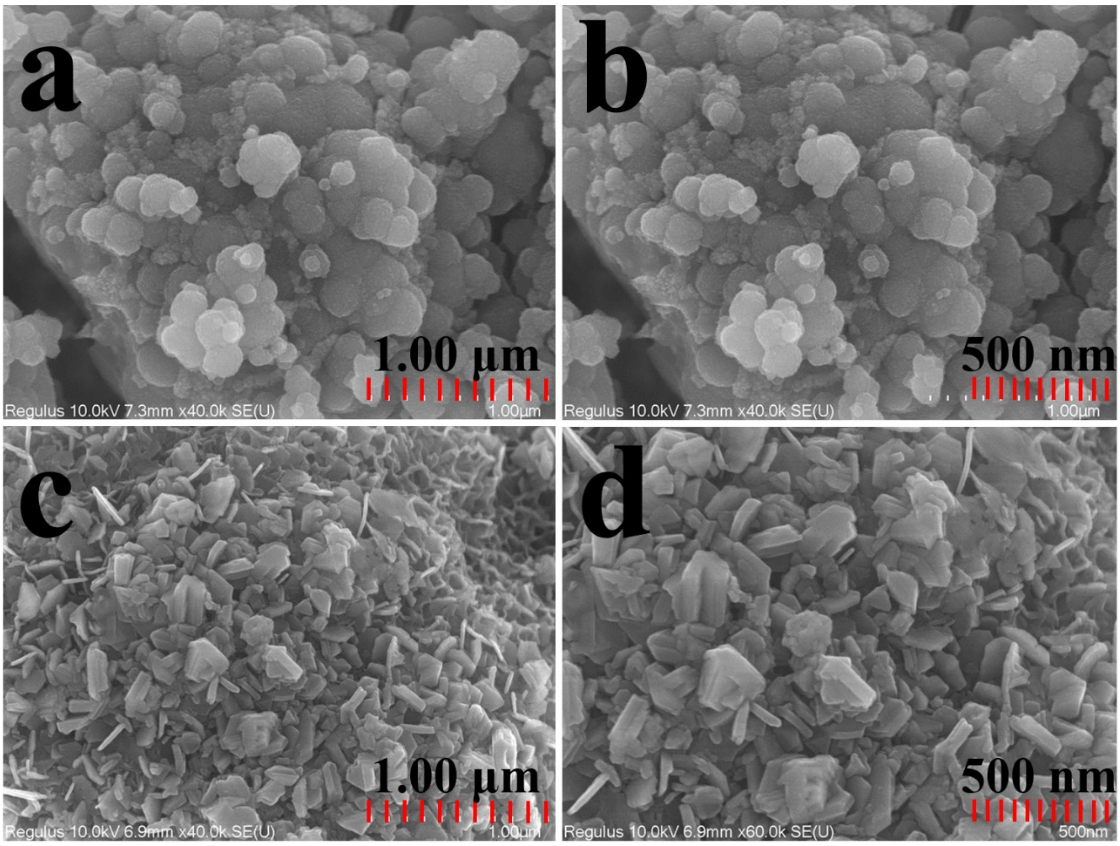

Fig. S4 The SEM image of Ni_3S_2@NiOOH/NF before and after HER stability test.

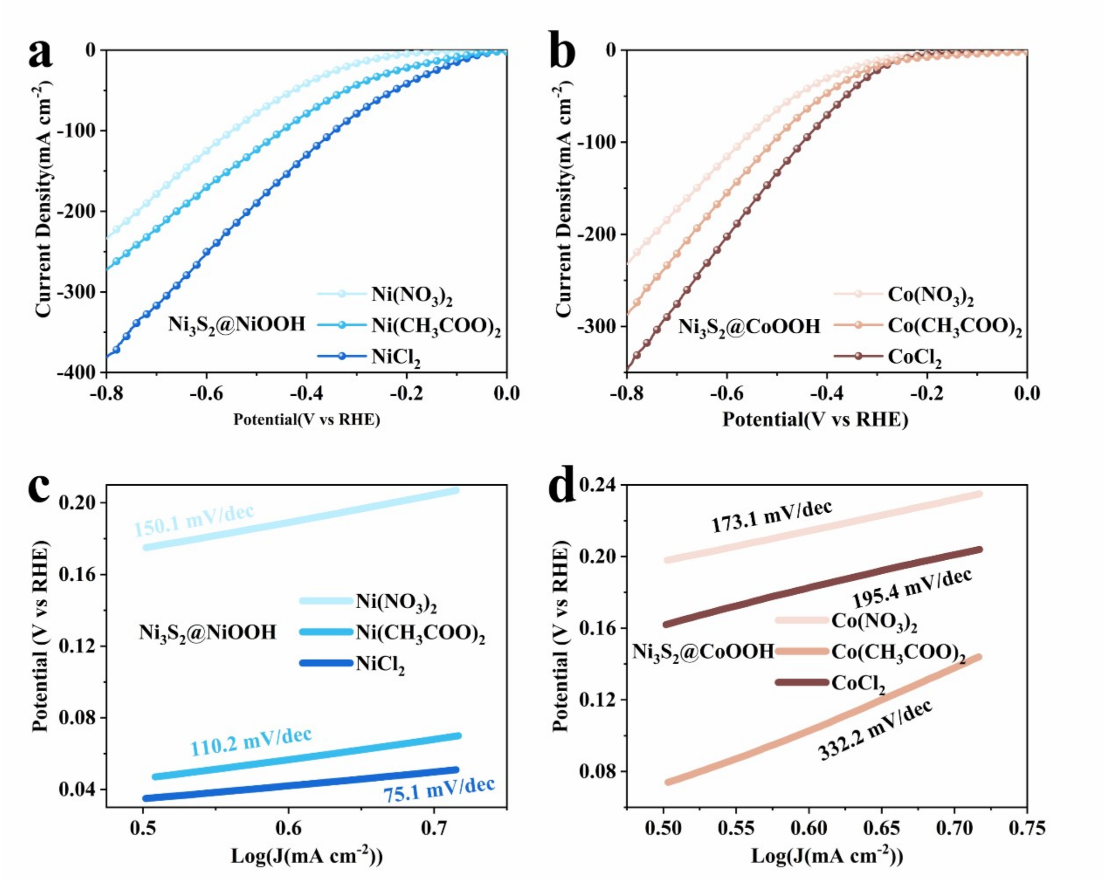

Fig. S5 The HER performance and Tafel slope of Ni_3S_2@NiOOH (a, c) and Ni_3S_2@CoOOH (b, d) samples prepared with different Ni and Co sources.

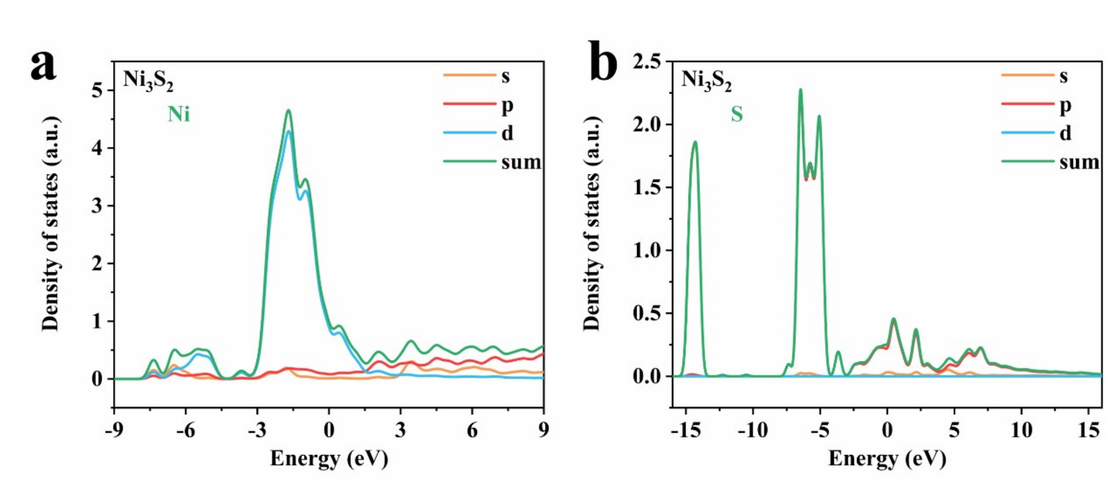

Fig. S6 Density of states for Ni_3S_2, (a) Ni and (b) S.

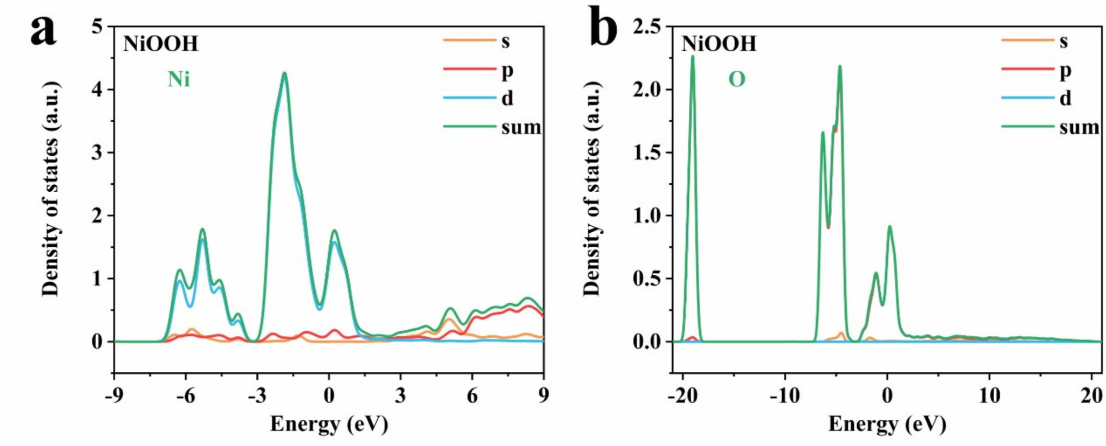

Fig. S7 Density of states for NiOOH, (a) Ni and (b) O.

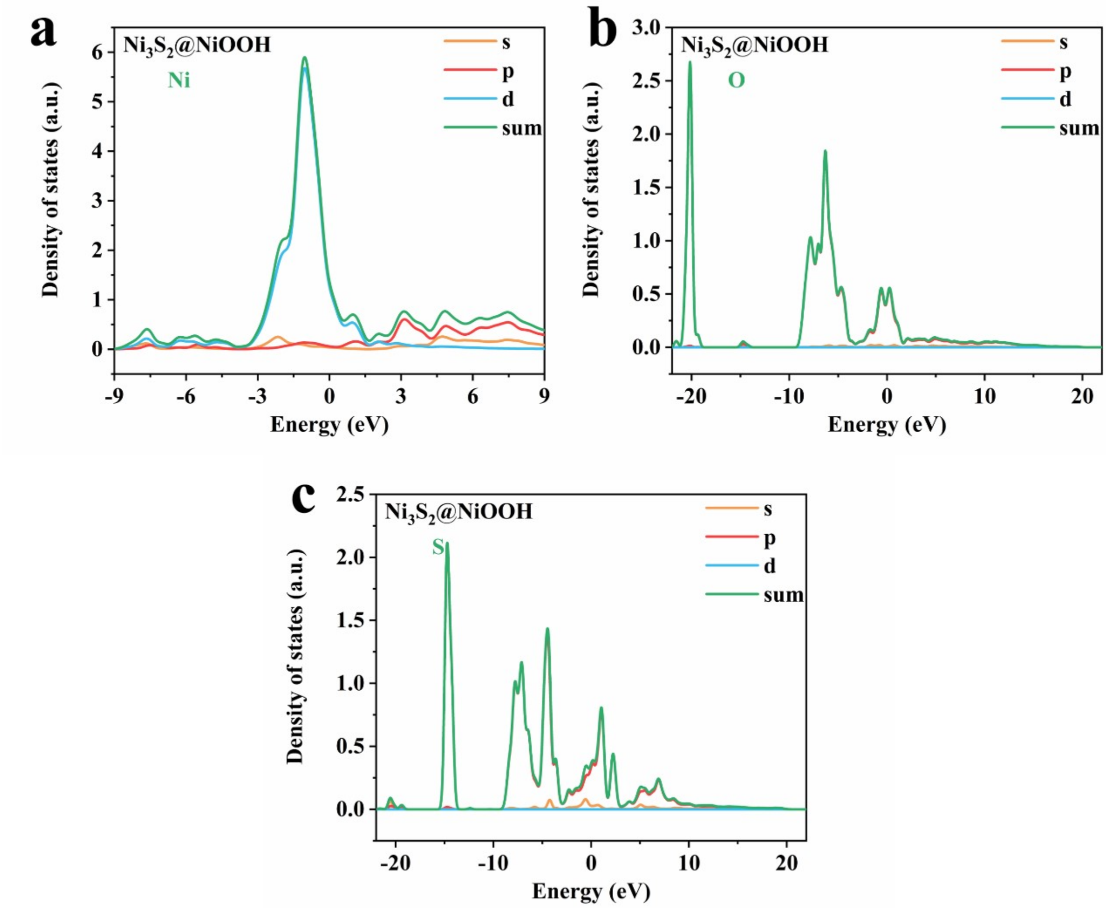

Fig. S8 Density of states for Ni_3S_2@NiOOH, (a) Ni, (b) O and (c) S.

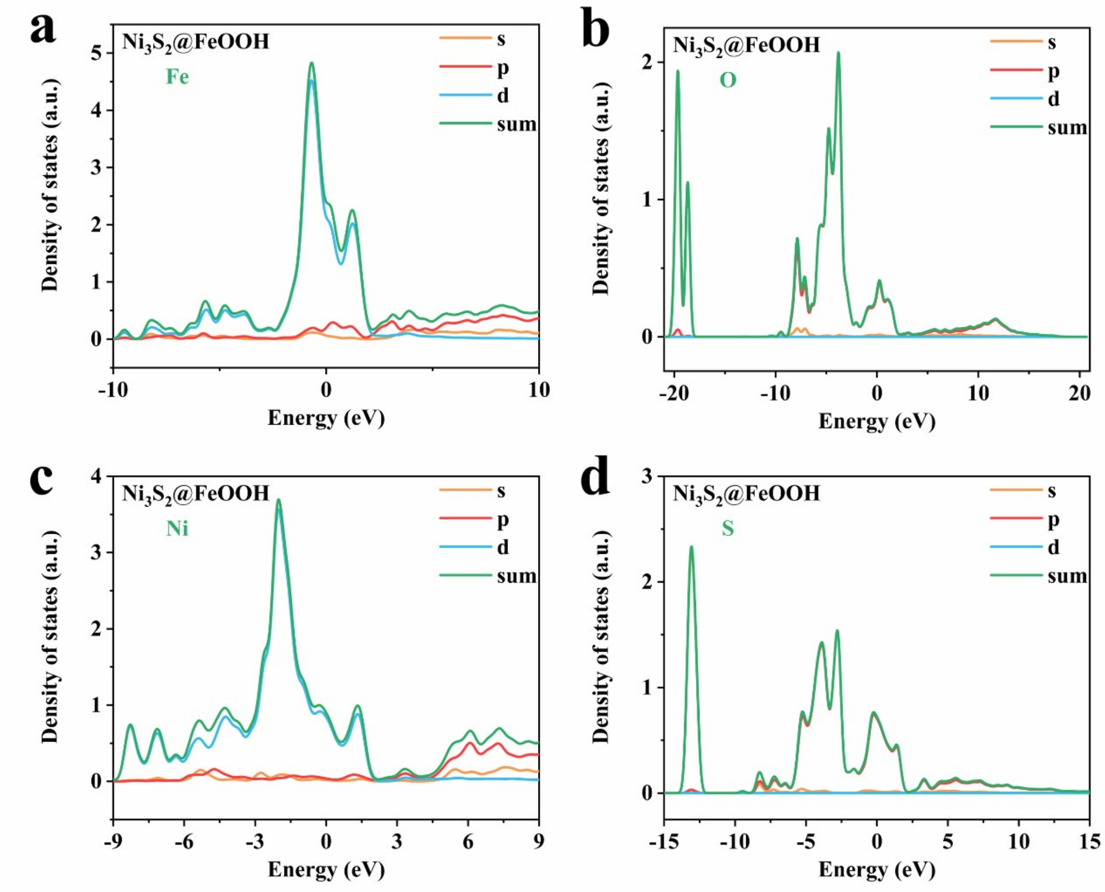

Fig. S9 Density of states for Ni_3S_2@FeOOH, (a) Fe, (b) O, (c) Ni, (d) S.

Table S1 HER performances and Tafel slope of Ni_3S_2@NiOOH/NF and other reported electrocatalysts in alkaline.

Catalyst	electrolyte	Overpotential at 10 mA/cm^2	Tafel slope (mV/dec)	Ref.
Ni_3S_2@NiOOH/NF	1.0 M KOH	79	75.1	This work
Ni_3S_2-$CoMoS_x$/NF	1.0 M KOH	234	125	[1]
Ni_3S_2/VG@NiCo LDHs	1.0 M KOH	120	87	[2]
Co_3O_4@Mo-Co_3S_4-Ni_3S_2/NF	1.0 M KOH	116	97	[3]
SnS-Ni_3S_2/NF	1.0 M KOH	145	86	[4]
Fe-Mo-S/Ni_3S_2@NF	1.0 M KOH	141	123	[5]
$CoNi_2S_4$/Ni_3S_2@NF	1.0 M KOH	171	88.6	[6]
Ni_3S_2@CoAl-LDHs	1.0 M KOH	175	108	[7]
CoS_x-Ni_3S_2/NF	1.0 M KOH	102	141	[8]
Co_9S_8-Ni_3S_2/NF	1.0 M KOH	215	171.2	[9]
a-MoS_2-Ni_3S_2/NF	1.0 M KOH	81	90.7	[10]
NiFe LDH@Ni_3S_2/NF	1.0 M KOH	184	115	[11]

Reference

[1]. Zhao, L.; Ge, H.; Zhang, G.; Wang, F.; Li, G., Hierarchical Ni_3S_2-$CoMoS_x$ on the nickel foam as an advanced electrocatalyst for overall water splitting. *Electrochim. Acta* **2021,** *387*, 138538.

[2]. Zhang, X.; Fan, J.; Lu, X.; Han, Z.; Cazorla, C.; Hu, L.; Wu, T.; Chu, D., Bridging NiCo layered double hydroxides and Ni_3S_2 for bifunctional electrocatalysts: The role of vertical graphene. *Chem. Eng. J.* **2021,** *415*, 129048.

[3]. Wu, Q.; Dong, A.; Yang, C.; Ye, L.; Zhao, L.; Jiang, Q., Metal-organic framework derived Co_3O_4@Mo-Co_3S_4-Ni_3S_2 heterostructure supported on Ni foam for overall water splitting. *Chem. Eng. J.* **2021,** *413*, 127482.

[4]. Zang, X.; Teng, J.; Zhang, X.; Guo, J., Heterogeneous SnS-Ni_3S_2 nanostructure for efficient overall water splitting. *Mater. Lett.* **2021,** *287*, 129290.

[5]. Zhang, Y.; Guo, H.; Li, X.; Du, J.; Ren, W.; Song, R., A 3D multi-interface structure of coral-like Fe-Mo-S/Ni_3S_2@NF using for high-efficiency and stable overall water splitting. *Chem. Eng. J.* **2021,** *404*, 126483.

[6]. Dai, W.; Ren, K.; Zhu, Y.-a.; Pan, Y.; Yu, J.; Lu, T., Flower-like $CoNi_2S_4$/Ni_3S_2 nanosheet clusters on nickel foam as bifunctional electrocatalyst for overall water splitting. *J. Alloy. Compd.* **2020,** *844*, 156252.

[7]. Du, Y.; Lu, Y.; Zhang, H.; Nie, Z.; Sun, Z.; Han, C.; Li, R.; Zhu, J., Facile Synthesis of Three-dimensional Hierarchical Ni_3S_2@CoAl-LDHs Nanosheet Arrays and Their Efficient Hydrogen Evolution. *ChemCatChem* **2020,** *12* (24), 6401-6409.

[8]. Jiang, L.; Yang, N.; Yang, C.; Zhu, X.; Jiang, Y.; Shen, X.; Li, C.; Sun, Q., Surface wettability engineering: CoS_x-Ni_3S_2 nanoarray electrode for improving overall water splitting. *Appl. Catal., B* **2020,** *269*, 118780.

[9]. Illathvalappil, R.; Walko, P. S.; Kanheerampockil, F.; Bhat, S. K.; Devi, R. N.; Kurungot, S., Hierarchical Nanoflower Arrays of Co_9S_8-Ni_3S_2 on Nickel Foam: A Highly Efficient Binder-Free Electrocatalyst for Overall Water Splitting. *Chem. - Eur. J.* **2020,** *26* (35), 7900-7911.

[10]. Song, S. W.; Wang, Y. H.; Li, W.; Tian, P. F.; Zhou, S. Y.; Gao, H. W.; Tian, X. Q.; Zang, J. B., Amorphous MoS_2 coated Ni_3S_2 nanosheets as bifunctional electrocatalysts for high-efficiency overall water splitting. *Electrochim. Acta* **2020,** *332*, 9.

[11]. Liang, X. Q.; Li, Y. H.; Fan, H.; Deng, S. J.; Zhao, X. Y.; Chen, M. H.; Pan, G. X.; Xiong, Q. Q.; Xia, X. H., Bifunctional NiFe layered double hydroxide@Ni_3S_2 heterostructure as efficient electrocatalyst for overall water splitting. *Nanotechnol.* **2019,** *30* (48), 9.